

# DEUTSCHES ELEKTRONEN-SYNCHROTRON **DESY**

DESY 74/17  
April 1974



A Coupled Channel Analysis of the Reactions  $\gamma\gamma \rightarrow \pi\pi$  and  $\gamma\gamma \rightarrow K\bar{K}$

by



K. Sundermeyer

*II. Institut für Theoretische Physik der Universität Hamburg*

**2 HAMBURG 52 · NOTKESTIEG 1**

A Coupled Channel Analysis of the Reactions  $\gamma\gamma \rightarrow \pi\pi$  and  $\gamma\gamma \rightarrow K\bar{K}$

Dissertation  
zur Erlangung des Doktorgrades  
des Fachbereichs Physik  
der Universität Hamburg

vorgelegt von  
Kurt Sundermeyer

aus  
Marienhafen

Hamburg

1974

---

Genehmigt vom Fachbereich Physik der Universität Hamburg auf Antrag von  
Prof. Dr. G. Kramer

Hamburg, den 12.12.1973

Prof. Dr. R. Haensel

Abstract

The processes  $\gamma\gamma \rightarrow \pi\pi$  and  $\gamma\gamma \rightarrow K\bar{K}$  are calculated using dispersion relation methods. The integral over the left hand cut is approximated by exchange of vector mesons. For the right hand cut unitarity is used including two-pion and two-kaon intermediate states. Coupling occurs in the  $I=0$  S-wave in a form recently given by a Berkeley group (Protopopescu et al.) and in the corresponding D-wave by a K-matrix with poles at the  $f(1270)$  and  $f'(1514)$ . Those cross sections for  $\pi\pi$  final states, in which the S-wave contributes, show a very marked spike at the  $K\bar{K}$ -threshold; those for  $\gamma\gamma \rightarrow K\bar{K}$  are of the order of  $\gamma\gamma \rightarrow \pi\pi$ , depending on the form in which strong interaction is built into the model, and on the  $K^* K\gamma$  coupling constant.

## 1. INTRODUCTION

Several groups have emphasized the importance of the two-photon exchange mechanism in electron-positron (electron) colliding beam physics [1]. This annihilation process, shown in Fig. 1, occurs in the form

$$e + e \rightarrow e + \gamma^* + e + \gamma^* \rightarrow e + e + X, \quad (1)$$

where X is a  $C=+1$  hadron state. The Weizsäcker-Williams equivalent photon approach [2] indicates that the cross sections for this type of reactions are dominant in the low c.m. energy range of the two photons. Therefore single hadron production (e.g.  $\pi^0$  and  $\eta$ ) and pion pair production should be the important final states.\* Since photon-photon annihilation offers a possibility to study meson pair production undisturbed by other hadronic channels, several models have been given for the process  $\gamma\gamma \rightarrow \pi\pi$  [4-6].

New phase shift analysis show that  $\pi\pi$  partial-waves are very much influenced by the opening of the  $K\bar{K}$ -channel at 990 MeV [7-8]. We therefore investigate the processes  $\gamma\gamma \rightarrow \pi\pi$  and  $\gamma\gamma \rightarrow K\bar{K}$  in a coupled model, using essentially the dispersive methods of Ref. [5]. Partial-wave dispersion relations are written down, where the left hand cut integral is approximated by  $\rho$ - and  $\omega$ -exchange (in the  $\pi\pi$ -case) and  $K^*$ -exchange ( $K\bar{K}$ -case). On the right hand cut inelastic unitarity is used. The resulting system of coupled singular integral-equations is solved by an iteration procedure.

The dispersion relations and the integral-equations are given in Sec. 2, the difficulties of solving them and the iteration scheme are presented in Sec. 3. In Sec. 4 the parametrization of the strong interaction part is described and the results of the calculations are compared with other findings [9-10]. In Sec. 5 we add some concluding remarks and discuss several objections, which can be made against the model.

---

\* For a review of photon-photon physics see Ref. [3].

## 2. AMPLITUDES AND DISPERSION RELATIONS

For the process  $\gamma\gamma \rightarrow \bar{M}M$  with real photons and a final state of two scalar or pseudoscalar mesons  $M$  (Fig.2) there are two invariant amplitudes<sup>\*</sup>

$$T = \left\{ \varepsilon_1 \cdot \varepsilon_2 - \frac{\varepsilon_1 \cdot k_2 \varepsilon_2 \cdot k_1}{k_1 \cdot k_2} \right\} T^{(1)} + \left\{ \varepsilon_1 \cdot k_2 \varepsilon_2 \cdot k_1 \frac{1}{2} \left( s - \frac{(t-u)^2}{s} \right) + \varepsilon_1 \cdot q_1 \varepsilon_2 \cdot q_2 (u-t-s) + \varepsilon_1 \cdot q_2 \varepsilon_2 \cdot q_1 (t-u-s) \right\} T^{(2)}, \quad (2)$$

where  $s=(k_1+k_2)^2$ ,  $t=(q_1-k_1)^2$  and  $u=(q_2-k_1)^2$ . The amplitude  $T$  is related to the cross section by

$$\frac{d\sigma_{\bar{M}M}}{d\Omega} = \frac{1}{64\pi^2 s} \sqrt{\frac{s-s_M}{s}} |T|^2, \quad (3)$$

where  $s_M=(2m_M)^2$ ,  $m_M$  the mass of the final state meson.<sup>\*\*</sup> Following Ref.[11] we can define s-channel helicity amplitudes free of kinematical singularities and giving the correct Thomson-limit ( $s \rightarrow 0$ ,  $m_M \rightarrow 0$ ) by

$$M_{++} = \frac{T_{++}}{s} = \frac{1}{s} \left\{ T^{(1)} - (tu - m_M^4) T^{(2)} \right\},$$

$$M_{+-} = \frac{T_{+-}}{tu - m_M^4} = T^{(2)}, \quad (4)$$

where the indices  $++$  and  $+-$  stand for equal and opposite orientied photon helicities. A decomposition into partial-wave amplitudes gives

$$M_{++} = 2\pi \sum_{J=0}^{\infty} (2J+1) f_+^J(s) d_{00}^J(\vartheta),$$

$$M_{+-} = 2\pi \sum_{J=0}^{\infty} (2J+1) f_-^J(s) \frac{d_{20}^J(\vartheta)}{1 - \cos^2 \vartheta}. \quad (5)$$

To simplify the unitarity relations we work with amplitudes of definite isospin  $I$

$$f_{\pi\pi}^{I=0}(s) = \frac{1}{\sqrt{3}} \left\{ 2 f_{\pi\pi}^c + f_{\pi\pi}^n \right\},$$

$$f_{\pi\pi}^{I=2}(s) = \sqrt{\frac{2}{3}} \left\{ f_{\pi\pi}^c - f_{\pi\pi}^n \right\},$$

$$f_{K\bar{K}}^{I=0}(s) = \frac{1}{\sqrt{2}} \left\{ f_{K\bar{K}}^c + f_{K\bar{K}}^n \right\},$$

$$f_{K\bar{K}}^{I=1}(s) = \frac{1}{\sqrt{2}} \left\{ f_{K\bar{K}}^c - f_{K\bar{K}}^n \right\}, \quad (6)$$

\* For the kinematic and definition of amplitudes see Ref.[5].

\*\*  $\hbar=c=1$ , in the following also  $m_\pi=1$ .

where c and n refer to charged and neutral final particles. The subscripts for spin and helicity will be omitted in the following and the indices 1 and 2 stand for the  $\pi\pi$  and  $K\bar{K}$ -channel. The dispersion relations are

$$\begin{aligned} f_1(s) &= f_1^B(s) + \frac{1}{\pi} \int_{-\infty}^s ds' \frac{\text{Im} f_1(s')}{s' - s - i\epsilon} + \frac{1}{\pi} \int_+^{\infty} ds' \frac{\text{Im} f_1(s')}{s' - s - i\epsilon} , \\ f_2(s) &= f_2^B(s) + \frac{1}{\pi} \int_{-\infty}^s ds' \frac{\text{Im} f_2(s')}{s' - s - i\epsilon} + \frac{1}{\pi} \int_+^{\infty} ds' \frac{\text{Im} f_2(s')}{s' - s - i\epsilon} . \end{aligned} \quad (7)$$

Here  $f_i^B(s)$  is the projection of the pion (kaon) Born terms (Fig.3) and  $s_0$  the c.m. energy of the  $K\bar{K}$ -threshold. The integrals over the left hand cut are approximated by single meson exchange (Fig.4), i.e. exchange of  $\rho$ - and  $\omega$ -mesons in the  $\pi\pi$ -case and the  $K^*$ -meson in the  $K\bar{K}$ -case. To avoid subtractions in Eq.(7) we assume that these particles lie on Regge trajectories, resulting in a form factor to the elementary vector meson and  $K$  meson Born graphs.

In extension of an earlier work [5] we now take unitarity with two-pion and two-kaon intermediate states to relate  $\text{Im} f_i(s)$  in the right hand cut integrals to strong interaction. In matrix formulation it reads

$$\begin{aligned} \text{Im} f(s) &= F^*(s) \rho(s) f(s) , \\ \text{Im} F(s) &= F^*(s) \rho(s) F(s) , \end{aligned} \quad (8)$$

where  $f(s)$  is the two-component vector of  $f_1$  and  $f_2$  and  $\rho$  is the phase-space diagonal matrix

$$\rho(s) = \begin{pmatrix} \rho_1 \Theta(s-t) & 0 \\ 0 & \rho_2 \Theta(s-s_0) \end{pmatrix}, \quad \rho_1 = \left(\frac{s-t}{t}\right)^{1/2}, \quad \rho_2 = \left(\frac{s-s_0}{t}\right)^{1/2}. \quad (9)$$

$F(s)$  is the amplitude of strong interaction related to the S-matrix

$$S = 1 + 2i \rho^{1/2} F \rho^{1/2}, \quad (10)$$

and  $S$  can be expressed in its most general form by phases  $\delta_i$  and inelasticity  $\eta$

\* The Born terms and their modification can be found in Ref.[5].

$$S = \begin{pmatrix} \gamma e^{2i\delta_1} & x \\ x & \gamma e^{2i\delta_2} \end{pmatrix}, \quad x = i \sqrt{1-\gamma^2} e^{i(\delta_1+\delta_2)}. \quad (11)$$

Combining  $f_i^B(s)$  together with the contributions of vector meson and  $K^*$  exchange to new functions  $g_i(s)$  and using (8) the dispersion relations (7) read

$$f_1(s) = g_1(s) + \frac{1}{\pi} \int_4^\infty ds' \frac{\rho_1 F_{11}^*(s') f_1(s')}{s' - s - i\epsilon} + \frac{1}{\pi} \int_{s_0}^\infty ds' \frac{\rho_2 F_{12}^*(s') f_2(s')}{s' - s - i\epsilon} \quad (12a)$$

$$f_2(s) = g_2(s) + \frac{1}{\pi} \int_{s_0}^\infty ds' \frac{\rho_1 F_{21}^*(s') f_1(s')}{s' - s - i\epsilon} + \frac{1}{\pi} \int_{s_0}^\infty ds' \frac{\rho_2 F_{22}^*(s') f_2(s')}{s' - s - i\epsilon} \quad (12b)$$

This is a coupled system of two singular integral-equations for the partial-waves  $f_1(s)$  and  $f_2(s)$ .

### 3. SOLUTION OF THE INTEGRAL-EQUATIONS

The most extensive work on singular integral-equations has been done by Mushkelishvili [12]. The author points out, that in general a solution of a system of equations is not possible in a rigorous manner. However one may hope that physical cases are special enough to allow a solution. Various authors tried to solve singular integral-equation systems for form factors [13], but they failed essentially because of the occurrence of the phase-space matrix. To demonstrate this we write the system in matrix form

$$f(x) = h(x) + \frac{1}{i\pi} \int_L dx' \frac{H(x') f(x')}{x' - x - i\epsilon}, \quad (13)$$

and then following the line of Mushkelishvili [12] and Ommès [14] a function

$$\varphi(z) = \frac{1}{2\pi i} \int_L dx' \frac{H(x') f(x')}{x' - z} \quad (14)$$

is introduced, with

$$2\varphi(x+) = \frac{1}{i\pi} \int_L dx' \frac{H(x') f(x')}{x' - x - i\epsilon}, \quad (15)$$

$$\varphi(x+) - \varphi(x-) = H(x) f(x)$$

Using this function Eq.(13) can be changed to

$$\left[ 1 - 2H(x) \right] \varphi(x+) - \varphi(x-) = H(x)h(x) , \quad (16)$$

which shall be written with two matrices A and B

$$\varphi(x+) - H(x) \varphi(x-) = B(x)h(x) . \quad (17)$$

The next step would be to make a product ansatz  $\varphi(z) = \phi(z)T(z)$ , where  $\phi(z)$  is the solution of the so-called homogeneous Hilbert problem

$$\phi(x+) - H(x) \phi(x-) = 0 . \quad (18)$$

For one integral-equation only, where A is no longer a matrix, Eq.(18) can be solved by taking the logarithm of it

$$\ln \phi(x+) - \ln \phi(x-) = \ln H(x) , \quad (19)$$

and then

$$\ln \phi(z) = \frac{1}{2\pi i} \int_L dx' \frac{\ln H(x')}{x' - z} . \quad (20)$$

These steps are in the general case possible only after diagonalizing A by  $UAU^{-1} = M$ . Eq.(17) is then

$$U(x) \varphi(x+) - M(x) U(x) \varphi(x-) = U(x) B(x) h(x) \quad (21)$$

The important point is, that only if  $U(x)$  is sectionally holomorphic the function  $U\varphi(z)$  possesses this property, which is necessary to go from Eq.(19) to Eq.(20).

In the case of interest  $A = 1 + 2iF\rho$  and the square-roots in  $\rho$  introduce branch points, essentially violating the condition of holomorphy. But even with degenerate thresholds branch cuts occur, because using the relation  $A = \rho^{-1/2} S \rho^{1/2}$  one can see that the eigenvalues of S

$$\lambda_{1,2} = \frac{\eta}{2} \left( e^{2i\delta_1} + e^{2i\delta_2} \right) \pm \frac{1}{2} \left[ \eta^2 \left( e^{2i\delta_1} + e^{2i\delta_2} \right)^2 - 4e^{2i(\delta_1 + \delta_2)} \right]^{1/2} \quad (22)$$

have branch cuts for nonvanishing coupling ( $\eta(s) \neq 1$ ).



A completely different way to get the partial-waves avoiding the difficulties with the integral-equations would be the N/D-method. Starting with the unitarity relations (8) the ansatz  $F=N \cdot D^{-1}$  leads to

$$\text{Im} (f \cdot D) = 0 \quad . \quad (23)$$

The dispersion relation

$$D(s) [f(s) - g(s)] = - \frac{1}{\pi} \int ds' \frac{\text{Im} [D(s')] g(s')}{s' - s - i\epsilon} \quad , \quad (24)$$

(where  $g(s)$  is the left hand cut contribution to  $f$ ) expresses the partial-waves as a function of  $D(s)$ . - In the one-channel case  $D$  has the same phase as  $F^* = |F| e^{-i\delta}$ , so writing a dispersion relation for  $\ln D$  results in

$$D(s) = \exp \left\{ - \frac{1}{\pi} \int ds' \frac{\delta(s')}{s' - s - i\epsilon} \right\} \quad . \quad (25)$$

In the multichannel case the phase of the D-function is not simply related to  $F$ , so here is the problem to split a known F-matrix into an N and a D part. Formulated this way we would get a system of four coupled singular integral-equations, a problem one likes to avoid.

An approximate solution would be to identify the N-function with the K-matrix

$$K = F (1 + i\rho F)^{-1} \quad , \quad (26)$$

thereby fulfilling the condition  $\text{Im} D = -\rho N$ . The real part would then be given by dispersion relations.

We choose another approximation method, solving Eqs.(12) by an iteration procedure. In the first step the nondiagonal term in Eq.(12a) is neglected and we solve

$$\tilde{f}_1(s) = g_1(s) + \frac{1}{\pi} \int_+^{\infty} ds' \frac{\rho_1 F_{11}^*(s') \tilde{f}_1(s')}{s' - s - i\epsilon} \quad . \quad (27)$$

This means that one considers the  $\pi\pi$  intermediate state only, but inelasticity is included. The result is used for Eq.(12b)

\* There are some very special cases of K-matrix parametrization in which the problem can be solved in a closed way.

$$f_2(s) = \tilde{g}_2(s) + \frac{1}{\pi} \int_{s_0}^{\infty} ds' \frac{\rho_2 F_{22}^*(s') f_2(s')}{s' - s - i\epsilon}, \quad (28)$$

where  $\tilde{g}_2(s)$  is now the modified inhomogeneous term

$$\tilde{g}_2(s) = g_2(s) + \frac{1}{\pi} \int_{s_0}^{\infty} ds' \frac{\rho_1(s') F_{21}^*(s') \tilde{f}_1(s')}{s' - s - i\epsilon}. \quad (29)$$

The next step then would be to insert the solution for  $f_2(s)$  from Eq.(28) into Eq.(12a), etc.

Since this iteration method can only be done by computer and because of the immense amount of time needed for the principal-value integrations, we close the scheme by using unitarity again, namely

$$f_1(s) = \text{Re } \tilde{f}_1(s) + i \left[ F_{11}^* \rho_1 \tilde{f}_1(s) + F_{12}^* \rho_2 f_2(s) \right]. \quad (30)$$

The justification for making the first iteration step only is discussed in Sect.5.

The results are

$$\tilde{f}_1(s) = g_1(s) + e^{u_1(s)} \frac{1}{\pi} \int_{s_0}^{\infty} ds' \frac{e^{-u_1(s')} \rho_1(s') F_{11}^*(s') g_1(s')}{s' - s - i\epsilon}, \quad (31a)$$

$$f_2(s) = \tilde{g}_2(s) + e^{u_2(s)} \frac{1}{\pi} \int_{s_0}^{\infty} ds' \frac{e^{-u_2(s')} \rho_2(s') F_{22}^*(s') \tilde{g}_2(s')}{s' - s - i\epsilon}, \quad (31b)$$

$$u_k(x) = \frac{x}{2\pi i} \int dx' \frac{\ln [1 + 2i \rho_k(x') F_{kk}(x')]}{x' (x' - x - i\epsilon)}. \quad (31c)$$

and  $\tilde{g}_2(s)$  is given by Eq. (29).

## 4. CALCULATIONS

### 4.1 Left hand cut parametrization

The input parameters to the left hand cut approximation by meson exchange are their couplings and their trajectories. The coupling constant  $g_{\omega\pi\gamma}$  can be determined from the decay  $\omega \rightarrow \pi^0\gamma$  [15] giving  $g_{\omega\pi\gamma} = 0.112$  (in units  $m_{\pi}^{-1}$ ). SU(3) predicts [16]

$$g_{\rho\pi\gamma} = \frac{1}{3} g_{\omega\pi\gamma}, \quad (32)$$

$$g_{K^{*+}K^-\gamma} = \frac{1}{3} g_{\omega\pi\gamma}, \quad g_{K^{*0}K^0\gamma} = -\frac{2}{3} g_{\omega\pi\gamma}.$$

For  $g_{\rho\pi\gamma}$  the experimental upper limit [17] agrees fairly well with the value from (32). Bemporad et al. [18] give a width  $\Gamma(K^{*+} \rightarrow K^+\gamma) < 80$  keV, which leads to  $g_{K^{*+}K^-\gamma} = 0.04$ , a value which is somewhat larger than the SU(3) prediction. - We use  $\alpha_{K^*} = \alpha_{\omega} = \alpha_{\rho}(t) = .57 + 0.96 t$ , where the  $\rho$ -trajectory has been taken from a fit to pion nucleon charge exchange reactions [19]. The results don't change very much with a more realistic intercept of the  $K^*$ -trajectory.

### 4.2 Parametrization of $\pi\pi$ and $K\bar{K}$ amplitudes

Recently two new  $\pi\pi$ -phase shift analysis have been published [7-8]. The CERN-Munich group [8] looked at data from  $\pi^- p \rightarrow \pi^- \pi^+ n$ , where the  $\pi\pi$  energy is in the range 600-1900 MeV, the Berkeley group [7] fitted experimental results from the reactions  $\pi^+ p \rightarrow \pi^+ \pi^- \Delta^{++}$  and  $\pi^+ p \rightarrow K^+ K^- \Delta^{++}$  in the range from 550 to 1150 MeV. Both of these groups get a sharp rise of the  $\pi\pi$  (isospin 0) S-wave phase near the two-kaon threshold from 90 degrees at 900 MeV to  $\sim 180$  degrees at 1000 MeV. This steep increase can be interpreted in terms of a second sheet pole very near the  $K\bar{K}$  threshold (S). Besides, there is a second pole ( $\epsilon$ ) far away from the physical region. The analysis favours the "down" solution for energies above the  $\rho$ -mass, thus settling the former "up-down" ambiguity.

For the S-waves we use the parametrization of Protopopescu et al. [7], which is given in a 2x2 M-matrix (related to our K-matrix by  $M=K^{-1}$ ).

Concerning the I=2 waves (which only exist for  $\pi\pi$ ),  $\delta_0^2$  is taken from Le Guillou, Morel and Navelet [20], and  $\delta_2^2$  is neglected, because all the analysis indicate

that it is very small [7,8]. Because nothing is known about the isospin 1 phases, which occur for  $\bar{K}\bar{K}$ , we put  $\delta_J^1$  to zero.

The I=0 D-waves are parametrized by a K-matrix, which consists of poles at the f and f' meson mass. In general a K-matrix for two resonances  $m_1$  and  $m_2$ , decaying into two channels with partial widths  $\Gamma_{11}, \Gamma_{12}$  resp.  $\Gamma_{21}, \Gamma_{22}$  would have the elements

$$K_{jj} = m_j \Gamma_{jj} + m_2 \Gamma_{2j} \quad (j=1,2) \quad , \quad (33)$$

$$K_{12} = K_{21} = m_1 \Gamma_{11} + m_2 \Gamma_{12} \quad , \quad \Gamma_j^2 = \Gamma_{j1} \Gamma_{j2} .$$

This leads by (26) to a simple Breit-Wigner form if  $\Gamma_{12}=0=\Gamma_{21}$

$$T_{jj} = m_j \Gamma_{jj} \quad , \quad T_{12} = 0 . \quad (34)$$

The K-matrix could be modified by non pole terms to get a background to the pure resonance behaviour (this has been done in [8]). We don't make this refinement, because there are no data for  $\delta_2^0$  in the  $\bar{K}\bar{K}$  case and we are interested only in a rough prediction for  $\gamma\gamma \rightarrow \bar{K}\bar{K}$ . - The authors of [8] exclude a decay of the f' into two pions, but we want to look for the influence of a small coupling on the  $\gamma\gamma \rightarrow \bar{M}\bar{M}$  cross sections. Therefore the following two situations are considered

- (i) f' coupling to  $\bar{K}\bar{K}$  only  $(\Gamma_{21} = 0, \Gamma_{22} = \Gamma_{f'} = 0.4) \quad ,$
- (ii) f' coupling to  $\bar{K}\bar{K}$  and to  $\pi\pi$   $(\Gamma_{12} = 0.15 \Gamma_{f'} , \Gamma_{22} = 0.85 \Gamma_{f'}) \quad ,$

whereas the f meson is assumed to decay into  $\pi\pi$  only ( $\Gamma_{11} = \Gamma_f = 1.1, \Gamma_{12} = 0$ )\*. In our model the  $\pi\pi$ -amplitude has resonance behaviour in the f region and a minimum in elasticity at the f' mass.

#### 4.3 Cross sections for $\gamma\gamma \rightarrow \pi\pi$

The cross sections  $\sigma_{\pm}^{c,n}$  (referring to charged and neutral final pions and to photon helicities of the same (+) and opposite (-) directions) are shown in

\* The widths in (33) for the f meson is modified to give the correct scattering length, see Ref. [5].

Figs.5-10. - The S-wave contributes to  $\sigma_{+}^{c,n}$  (Figs.5-8) only. These cross sections have a very outstanding structure near the  $K\bar{K}$ -threshold, reflecting the fact that  $\delta_0^0$  increases very rapidly in that region. The magnitude of the spike depends strongly on the vector meson couplings as can be seen by comparing Figs. 5 and 7 with Figs. 6 and 8. The cross sections are somewhat sensitive to the magnitude of the  $K^*$  coupling, they are generally higher if  $K^*$  exchange is allowed. An  $f$  meson signal occurs in most of the curves, depending also on the coupling constants. The influence of the  $f'$  meson is small, if  $K^*$  couplings are zero. Besides these calculations we show for comparison the results of the one-channel calculation [5], where the S-wave has been parametrized by a Breit-Wigner ansatz for the  $\epsilon$  meson ("up" type solution) and the other waves are essentially the same (no coupling of  $f'$ ). Above  $\sim 1.1$  GeV the cross sections are nearly the same, but they have a structure in the  $\epsilon$ -meson region, which is no longer there in this coupled channel analysis.

The cross sections  $\sigma_{-}^{c,n}$  (Figs.9-10) don't change much when going from the one-channel model to the two-channel case.\* This is because only D-waves contribute, which are the same - apart from a possible coupling of the  $f'$  meson. The influence of the  $f'$  is stronger in  $\sigma_{-}^n$  than in  $\sigma_{-}^c$ , but  $\sigma_{-}^n$  is by one order of magnitude smaller than  $\sigma_{-}^c$ . We don't show the cross sections  $\sigma_{-}^n$  for the case of vanishing vector meson coupling, because they are nearly the same as if the couplings were included.

#### 4.4 Cross sections for $\gamma\gamma \rightarrow K\bar{K}$

These cross sections - with the same notation as in 4.3 - are shown in Figs.11-14. Comparing Fig. 11a with 11b and 12a with 12b one can see the big influence of  $K^*$  exchange for  $\sigma_{+}^{c,n}$ .  $\sigma_{+}^c$  is relatively flat, if  $K^*$  exchange is absent. In the case with  $K^*$  exchange it has a structure near the  $f'$  meson region, besides the maximum from the kaon Born term. The detailed form depends on the width  $\Gamma(f' \rightarrow K\bar{K})$  and the size of the  $\rho/\omega$  coupling constants. - The cross section  $\sigma_{+}^n$  is in the case with  $K^*$  exchange of the same order of magnitude as  $\sigma_{+}^c$  and nearly independent of the other details in parametrization. If  $g_{K^*K\pi} = 0$  it falls off by a factor of two in the considered energy range.

\* The cross sections for energies below .7 GeV can be found in [5].

The cross section  $\sigma_c$  is nearly stable with respect to changes in the parametrization. It has a striking dip in an interval of only  $\sim 50$  MeV at the  $f'$  meson mass, whereas  $\sigma_n$  shows a maximum (the same situation occurred for  $\sigma_c(\pi\pi)$  and  $\sigma_n(\pi\pi)$  in the  $f$  region).  $\sigma_n$  depends on the size of the  $K^*$  coupling, but it is very small compared to  $\sigma_c$ .

That the process  $\gamma\gamma \rightarrow K\bar{K}$  is more sensitive to  $K^*$  exchange, than  $\gamma\gamma \rightarrow \pi\pi$  is sensitive to vector meson exchange, becomes clear from the fact that the masses of  $K$  and  $K^*$  are not so much different than the masses of pions compared to  $\rho$  and  $\omega$  mesons.

#### 4.5 Comparison with other models

Also using dispersive methods, Isaev and Kleskov made a rough model for  $\gamma\gamma \rightarrow K\bar{K}$  [9], assuming that in the unitarity relation (8) the two-pion state is the important one. In our notation they took for Eq. (12)  $F_{12}=0=F_{22}$  and used the one-channel solution  $f_1$  for  $\gamma\gamma \rightarrow \pi\pi$  to get  $f_2$  from Eq. (12b), which now is no longer an integral equation. Comparison with their results is not meaningful because they didn't use the new S-wave phase shift and approximated the D-wave for  $\gamma\gamma \rightarrow K\bar{K}$  by an  $f$  meson. We agree with their statement that the cross sections for  $\gamma\gamma \rightarrow K\bar{K}$  are of the order of  $\gamma\gamma \rightarrow \pi\pi$ . However their approximation cannot be realistic in the  $f'$  region. Therefore we think that a structure in the  $K\bar{K}$  cross sections should occur at these energies and not in the  $f$  meson region, which these authors get because of their D-wave parametrization.

Gensini [10] calculated the partial waves by an iteration procedure similar to our method. He introduced a  $(R, \phi)$  representation instead of our  $(\eta, \delta)$  one, writing the unitarity Eq. (8) in the form

$$\begin{aligned} \text{Im } f_1(s) &= \tilde{R}_1(s) F_1^*(s) f_1(s) \\ \text{Im } F_1(s) &= R_1(s) |F_1(s)|^2 \end{aligned} \quad (35)$$

The assumption  $\text{Im } \tilde{R}_1=0$  implies the identity of  $\tilde{R}_1$  and  $R_1$ , and this means that the two-pion intermediate state is the dominant one. Gensini neglected the contribution of vector mesons in the crossed channels and investigated S-waves only, using the parametrization of Protopopescu et al. [7]. The results of [10] are comparable to those of our model for the general structure and order of magnitude only, because cross sections are not calculated in that work. Gensini predicts a spike for  $\sigma(\pi\pi)$  at the  $K\bar{K}$ -threshold too, and we agree with the magnitude of  $\gamma\gamma \rightarrow \pi\pi$  and  $\gamma\gamma \rightarrow K\bar{K}$  amplitudes.

## 5. CONCLUSIONS AND REMARKS

Some critical remarks are to be made concerning the reliability of the model. One point is that the solution of an Omnès equation is determined only up to a polynomial of degree  $n$ , if the strong interaction phase  $\delta$  grows up to  $n\pi$ , a freedom which corresponds to the possible appearance of CDD poles in  $N/D$  calculations. And just the most interesting  $\pi\pi$  S-wave phase  $\delta_0^0$  seems to go past  $180^\circ$ . \* Isaev and Kleskov have discussed, how this freedom affects the results for the one-channel calculations of  $\gamma\gamma \rightarrow \pi\pi$  [6].

Another open question is the form of the strong interaction phases for low energies. Carlson and Wu-Ki Tung have shown that it is the parametrization of the phases near the threshold that influences the form of the cross sections for  $ee \rightarrow ee\pi\pi$ , when instead of taking the equivalent photon approach, the exact formula is used [21].

Our model gives cross sections up to 1.6 GeV and one has to ask, if it is sufficient to take two-pion and two-kaon intermediate states only to describe inelasticity. Thus, the  $4\pi$  channel could contribute with  $\rho\rho$  states at 1.53 GeV, presumably changing the results on the structure of the cross sections in the  $f'$  region.

We don't have a control on the reliability of the iteration procedure. It rests on the assumption that  $\pi\pi$  interaction is mostly dominated by two-pion intermediate states. This condition is not fulfilled for the energy region near the  $K\bar{K}$  threshold, but we think that this is corrected by using unitarity in the final step of the iteration, see Eq.(30).

Notwithstanding these objections the rough structure of our calculations should remain valid. One of our results is, that the  $\gamma\gamma \rightarrow \pi\pi$  cross sections are very sensitive to the  $\pi\pi$  interaction. Already at energies greater than  $\sim 700$  MeV, where the Born contribution flattens out, the S-wave phase shifts can be studied. - The dependence of the cross sections on vector meson couplings is an outstanding fact, so measurements at higher energies of the two mesons can separate the different parameters in our model. This is especially true for the  $K\bar{K}$  final state, but the cross sections for  $ee \rightarrow ee+K\bar{K}$  are by two orders of magnitude smaller compared to  $ee \rightarrow ee+\pi\pi$ .

---

\* We fix this ambiguity by assuming that  $s.f(s) \rightarrow 0$  for  $s \rightarrow \infty$ .

In Ref. [5] the partial widths for  $\epsilon$  and  $f$  into two photons had been given. With the same assumptions we get  $(f' \rightarrow \gamma\gamma) = 0.5 \text{ keV}$ , but this value depends very strongly on the  $K^* K\gamma$  coupling constant.

The calculation can immediately be extended to virtual photons, but refining the model only makes sense if experimental data are available. We think that it should be possible to learn something about meson-meson dynamics from future storage ring experiments, when beam energies are high enough to pick up data from two-photon processes and statistics allows to separate the different cross sections  $\sigma_{\pm}^{c,n}$ . As mentioned in Ref. [5] this can be done by measuring  $d\sigma_{\gamma\gamma}/d\Omega$  at least at 3 different angles.

The author thanks Professor G. Kramer for helpful discussions and Dr. G. Schierholz for discussions in the early phase of this work.



REFERENCES

- [1] S.J. Brodsky, T. Kinoshita and H. Terazawa, Phys.Rev.Lett. 25 (1970) and Phys.Rev. D4 (1971) 1532;  
V.M. Budnev and I.F. Ginzburg, Soviet Phys. JETP Lett 12 (1970) 238;  
N. Arteaga-Romero, A. Jaccarini and P. Kessler, Phys.Rev. D3 (1971) 1569.
- [2] C.F. Weizsäcker, Z.Physik 88 (1934) 612;  
E.J. Williams, Phys.Rev. 45 (1934) 729.
- [3] H. Terazawa, Rev.Mod.Phys. 45 (1973) 615.
- [4] F. Calogero and C. Zemach, Phys.Rev. 120 (1960) 1860;  
P.C. De Celles and J.F. Goehl, Jr., Phys.Rev. 184 (1969) 1617;  
D.H. Lyth, Nucl.Phys. B30 (1971) 195;  
C.E. Carlson and Wu-Ki Tung, Phys.Rev. D4 (1971) 2873;  
R. Goble and J. Rosner, Phys.Rev. D5 (1972) 2345;  
F.J. Yndurain, Nuovo Cim. 7A (1972) 687;  
P.S. Isaev and V.I. Kleskov, Reaction  $\gamma\gamma \rightarrow \pi\pi$  and pion electromagnetic mass difference, Dubna preprint JINR E2-6527 (June, 1972).
- [5] G. Schierholz and K. Sundermeyer, Nucl.Phys. B40 (1971) 125.
- [6] P.S. Isaev and V.I. Kleskov, The effect of the choice of the  $\pi\pi$  scattering phase parametrization on the  $\gamma\gamma \rightarrow \pi\pi$  and  $\gamma\gamma \rightarrow \gamma\gamma$  reaction cross section, Dubna preprint JINR P2-6943 (February, 1973), in russian.
- [7] S.D. Protopopescu, M. Alston-Garnjost, A. Barbaro-Galtieri, S.M. Flatté, J.H. Friedman, T.A. Lasinski, G.R. Lynch, M.S. Rabin and F.T. Solmitz, Phys. Rev. D7 (1973) 1279.
- [8] B. Hyams, C. Jones, P. Weilhammer, W. Blum, H. Dietl, G. Grayer, W. Koch, E. Lorenz, G. Lütjens, W. Männer, J. Meissburger, W. Ochs, U. Stierlin, and F. Wagner, Nucl. Phys. B64 (1973) 134.
- [9] P.S. Isaev and V.I. Kleskov, Investigation of reactions  $\gamma\gamma \rightarrow \bar{K}K$  and  $\gamma\gamma \rightarrow \gamma\gamma$  by the method of dispersion relations, Dubna preprint JINR E2-6666 (January, 1972).

- [10] P. Gensini, A treatment of meson pair production in  $\gamma\gamma$  collisions including inelasticity and current algebra, Lecce Univ. Preprint UL/IF-7-72/73 (July, 1973).
- [11] H.D.I. Abarbanel and M.L. Goldberger, Phys.Rev. 165 (1968) 1594.
- [12] N.I. Mushkelishvili, Singular Integral Equations (Noordhoff, Groningen, 1953) 324 ff.
- [13] T.F. Walsh, Nuovo Cim. 68A (1970) 469;  
L. Resnick, Phys. Rev. D2 (1970) 1975;  
H.J. Kreuzer and A.N. Kamal, Phys.Rev.D6 (1972) 1638.
- [14] R. Omnès, Nuovo Cim. 8 (1958) 316.
- [15] PARTICLE DATA GROUP, Rev.Mod.Phys. 45 (1973) S155.
- [16] M. Gourdin, Unitary Symmetries (North-Holland, Amsterdam, 1967) 95 f.
- [17] R. Erbe et al. (Aachen-Berlin-Bonn-Hamburg-Heidelberg-München Collab.), Phys.Rev. 188 (1969) 2060.
- [18] C. Bemporad et al., Nucl. Phys. B51 (1972) 1.
- [19] G. Höhler, J. Baacke and G. Eisenbeiss, Phys.Lett. 22 (1966) 203.
- [20] J.C. Le Guillou, A. Morel and H. Navelet, Nuovo Cim. 5A (1971) 659.
- [21] C.E. Carlson and Wu-Ki Tung, Phys.Rev. D6 (1972) 147.

FIGURE CAPTIONS

Fig. 1: Colliding beam production of a neutral  $C=+$ hadron state.

Fig. 2: The  $\gamma\gamma \rightarrow M\bar{M}$  Vertex.

Fig. 3: Pion (kaon) Born graphs.

Fig. 4: Crossed channel resonance contribution.

Fig. 5: The cross section  $\sigma_+^C$  for charged pions for the case of equal helicities, with vector meson exchange in the crossed channel.

Notation:

\_\_\_\_\_ with  $K^*$  exchange in the  $K\bar{K}$  channel and coupling in the (isospin 0) D-wave (case (ii)) described in the text,  
 - - - - - with  $K^*$  exchange, no coupling (case (i)),  
 - · - · - · - without  $K^*$  meson and case (ii),  
 - · - · - · - decoupled model with a resonance parametrization of the  $\rho$ -meson.

Fig. 6:  $\sigma_+^C$  without vector meson exchange. The notation is as in Fig. 5.

Fig. 7: The cross section  $\sigma_+^N$  for neutral pions with vector meson exchange. The details are as in Fig. 5.

Fig. 8:  $\sigma_+^N$  without vector mesons; notation as in Fig. 5.

Fig. 9: The cross section  $\sigma_-^C$  for charged pions in case of opposite photon helicities; Fig.9a - without vector meson exchange, Fig.9b - with vector mesons. The notation is as in Fig. 5.

Fig. 10: The cross section  $\sigma_-^N$  for neutral pions with vector meson exchange. Details are as in Fig. 5.

Fig. 11: The cross section  $\sigma_-^N$  for charged kaons in case of equal photon helicities; Fig.11a - with  $K^*$  exchange, Fig. 11b - without  $K^*$  mesons.

Notations:

\_\_\_\_\_ vector meson exchange in the  $\pi\pi$  channel and coupling in the (isospin) D-wave (case (ii)),  
 - - - - - with vector mesons, no coupling (case (i)),  
 - · - · - · - without vector mesons and case (ii),  
 - · - · - · - without vector mesons and case (i).

Fig. 12: The cross section  $\sigma_+^N$  for neutral kaons; Fig.12a - with  $K^*$  exchange, Fig. 12b - without  $K^*$  exchange and the notation is as in Fig. 11.

Fig. 13: The cross section  $\sigma_-^C$  for charged kaons in case of opposite helicities. Notation:

\_\_\_\_\_ with  $K^*$  exchange and coupling in the (isospin 0) D-wave (case (ii)),

- - - - - with  $K^*$ , no coupling (case (i)),  
-.-.-.-.- without  $K^*$  exchange and case (ii),  
-.-.-.-.- without  $K^*$  and case (i).

Fig. 14: The cross section  $\sigma_-^n$  for neutral kaons. Details are as in Fig. 13, but note the different scale.

## LEBENS LAUF

Kurt Sundermeyer

7.12.1943 geboren als erstes Kind des Vermessungstechnikers  
Heinrich Sundermeyer und seiner Ehefrau Else, geb.Poppinga,  
in Marienhaf e (Kreis Norden)

1950-54 Besuch der Volksschule in Emden

1954-63 Besuch des Gymnasiums für Jungen (math.-naturwiss. Zweig)  
Emden

Febr. 1963 Reifeprüfung

1963-65 Dienstzeit bei der Bundeswehr

SS 1965 Beginn des Studiums der Physik an der Universität Hamburg

WS 1969 Beginn der Diplomarbeit bei Herrn Prof. Dr. G. Kramer,  
II. Institut für Theoretische Physik, Universität Hamburg;  
Thema: Untersuchung über das Verhalten des  $A^+$ -Anteils  
der Pion-Nukleon Streuung bei hohen Energien.

Okt. 1969 Heirat mit Barbara Mahler

WS 1970/71 Diplomhauptprüfung

15.2.1971- Wissenschaftliche Hilfskraft am II. Institut für Theore-  
tische Physik, Universität Hamburg

31.1.1973

seit 1.2.1973 Wissenschaftlicher Angestellter ebenda

Dez. 1973 Doktorprüfung beim Fachbereich Physik, Universität Hamburg

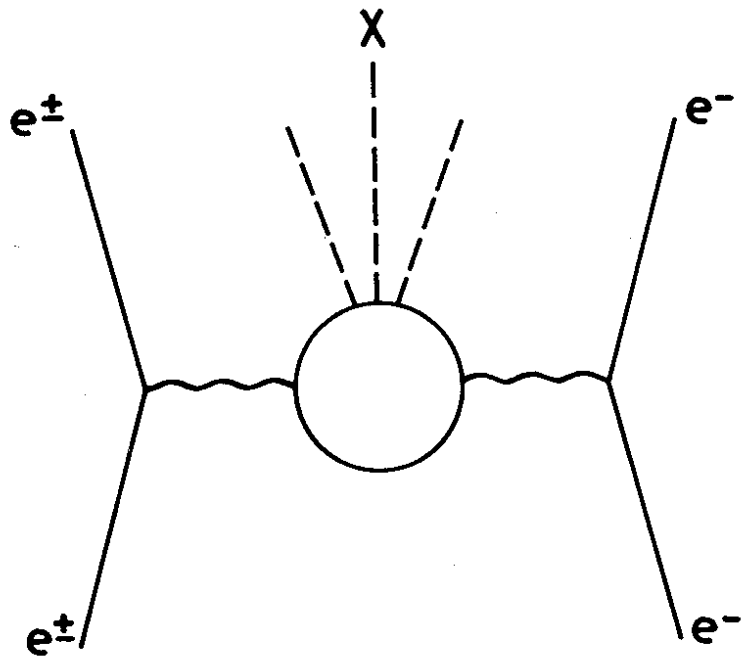


Fig. 1

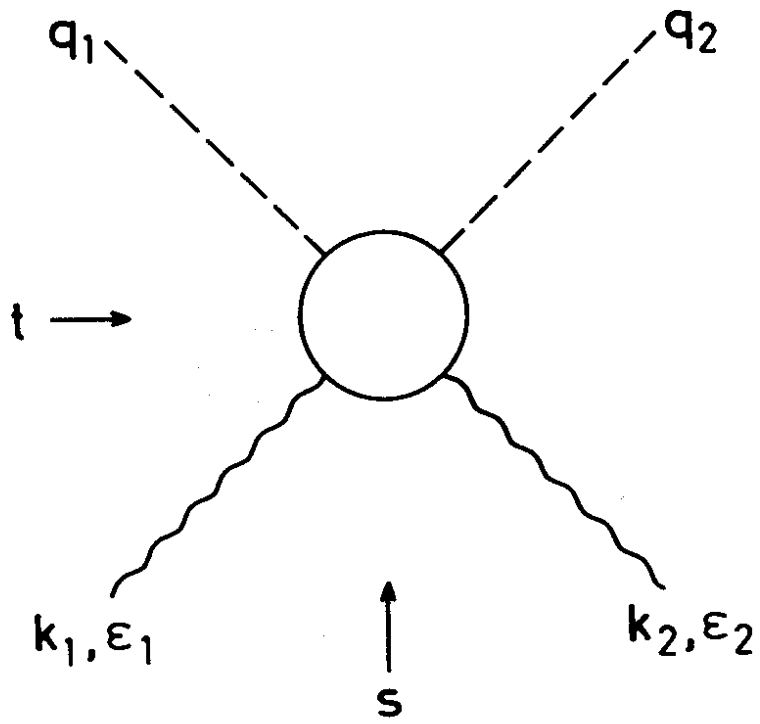


Fig. 2

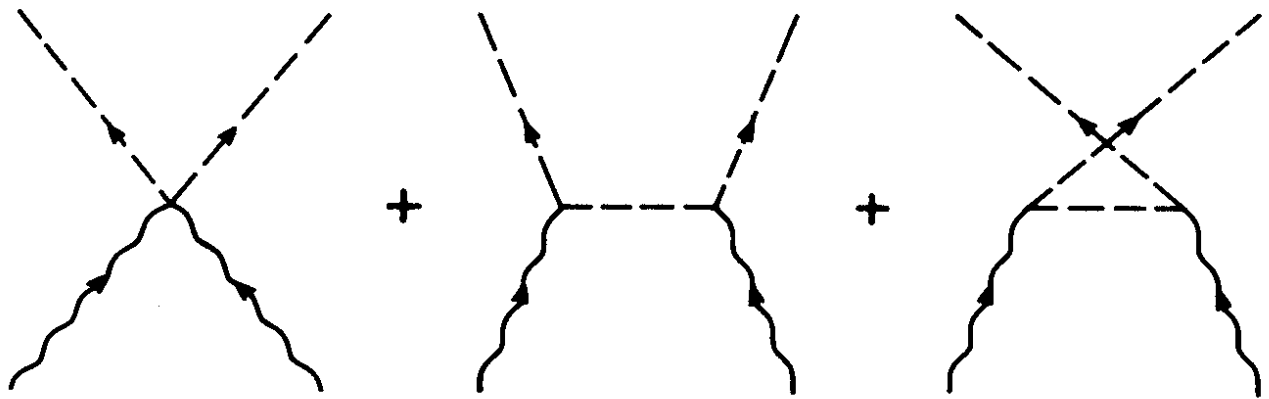


Fig. 3

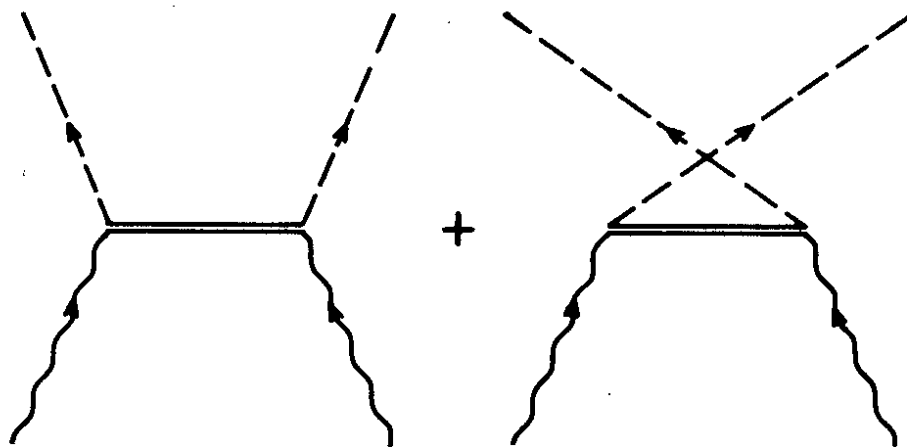


Fig. 4

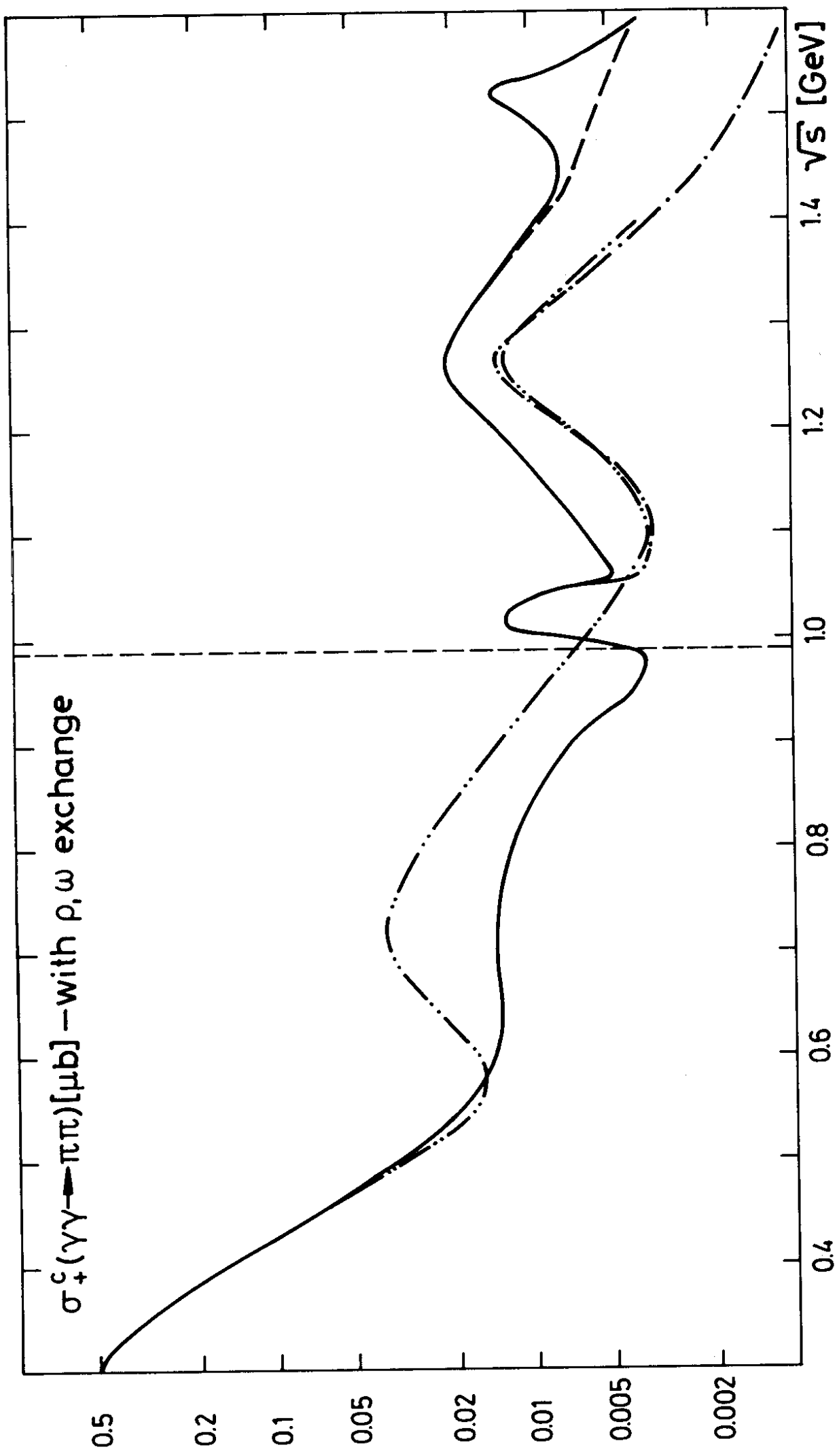


Fig. 5



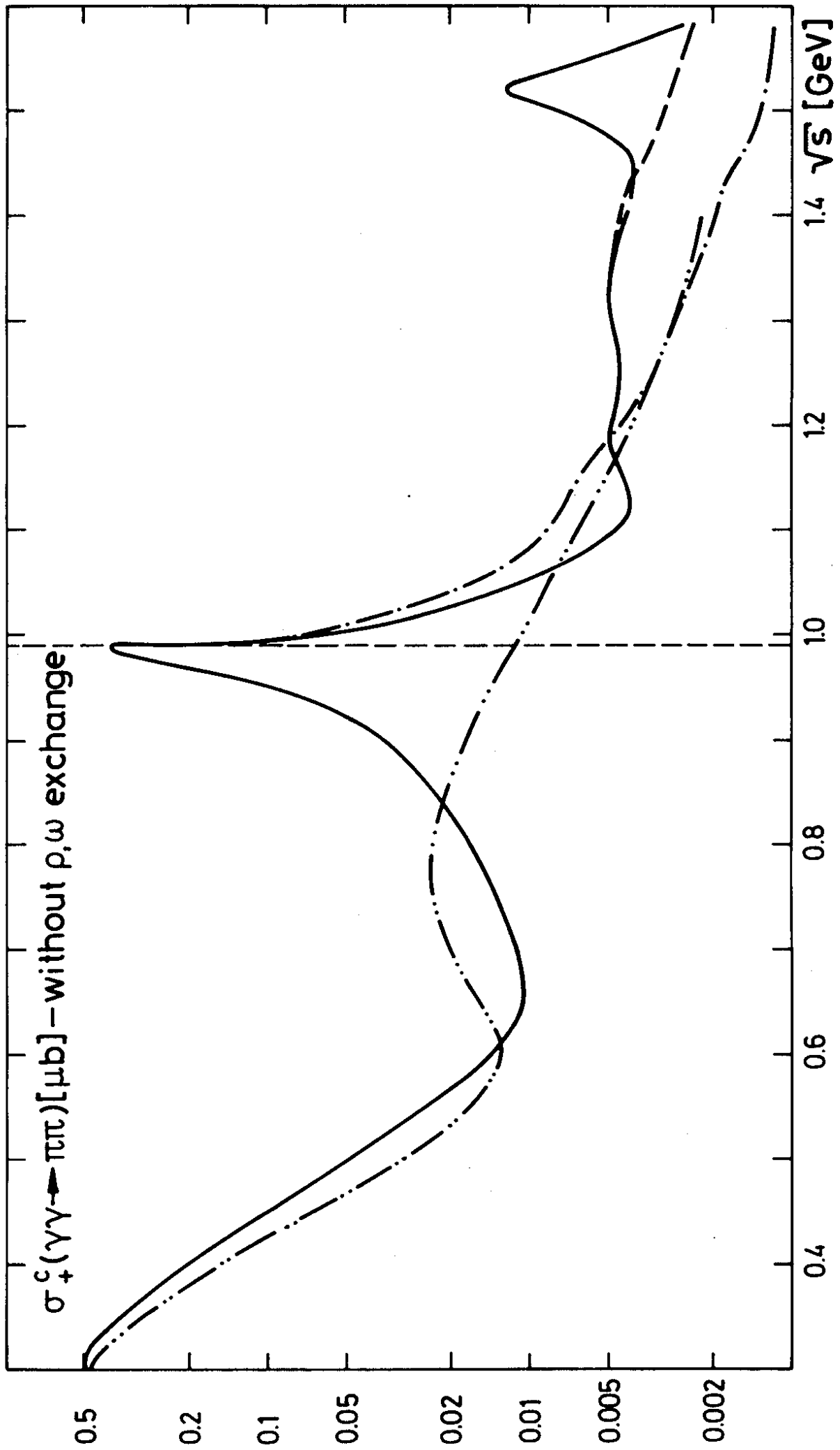


Fig. 6

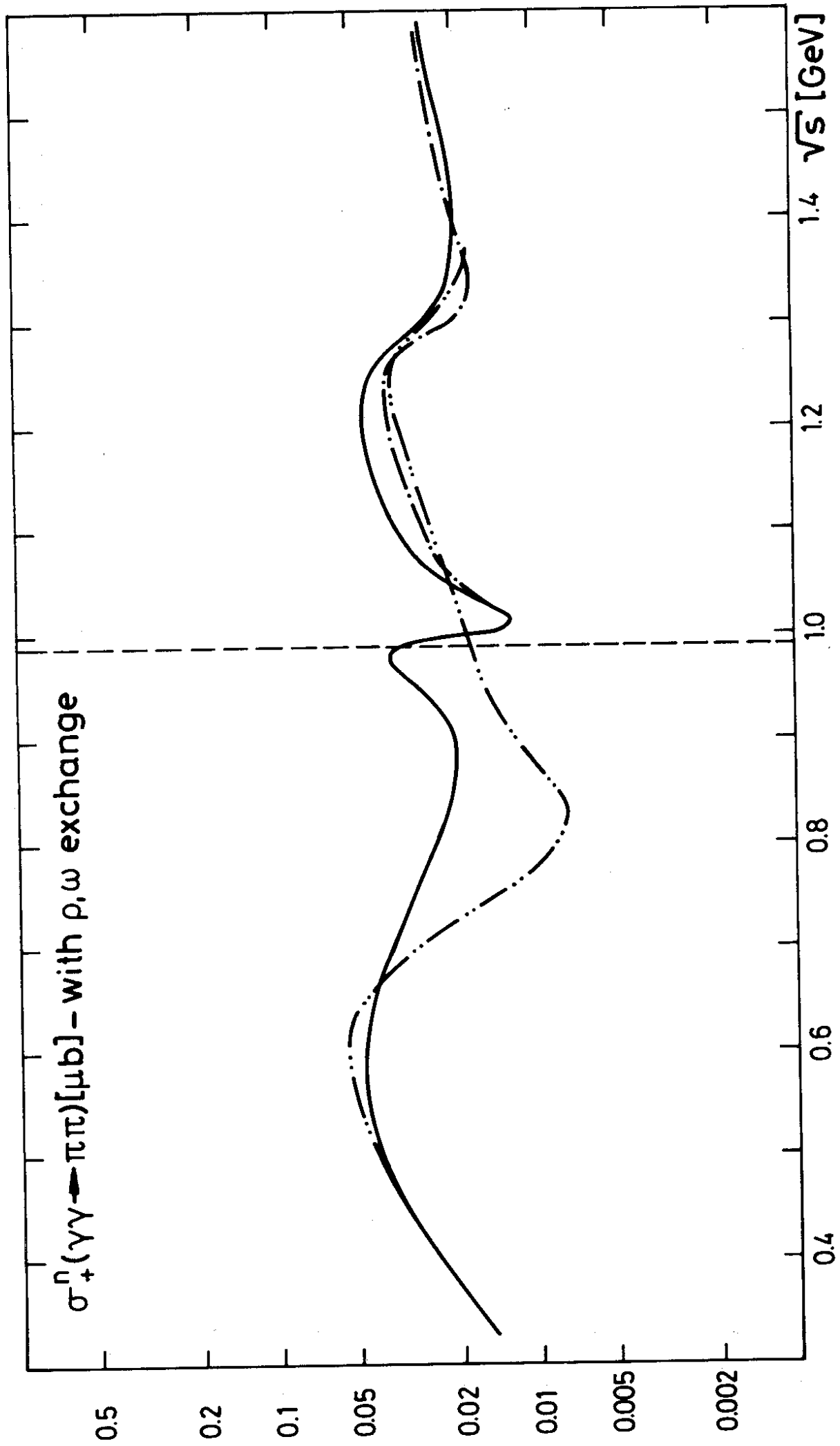


Fig. 7

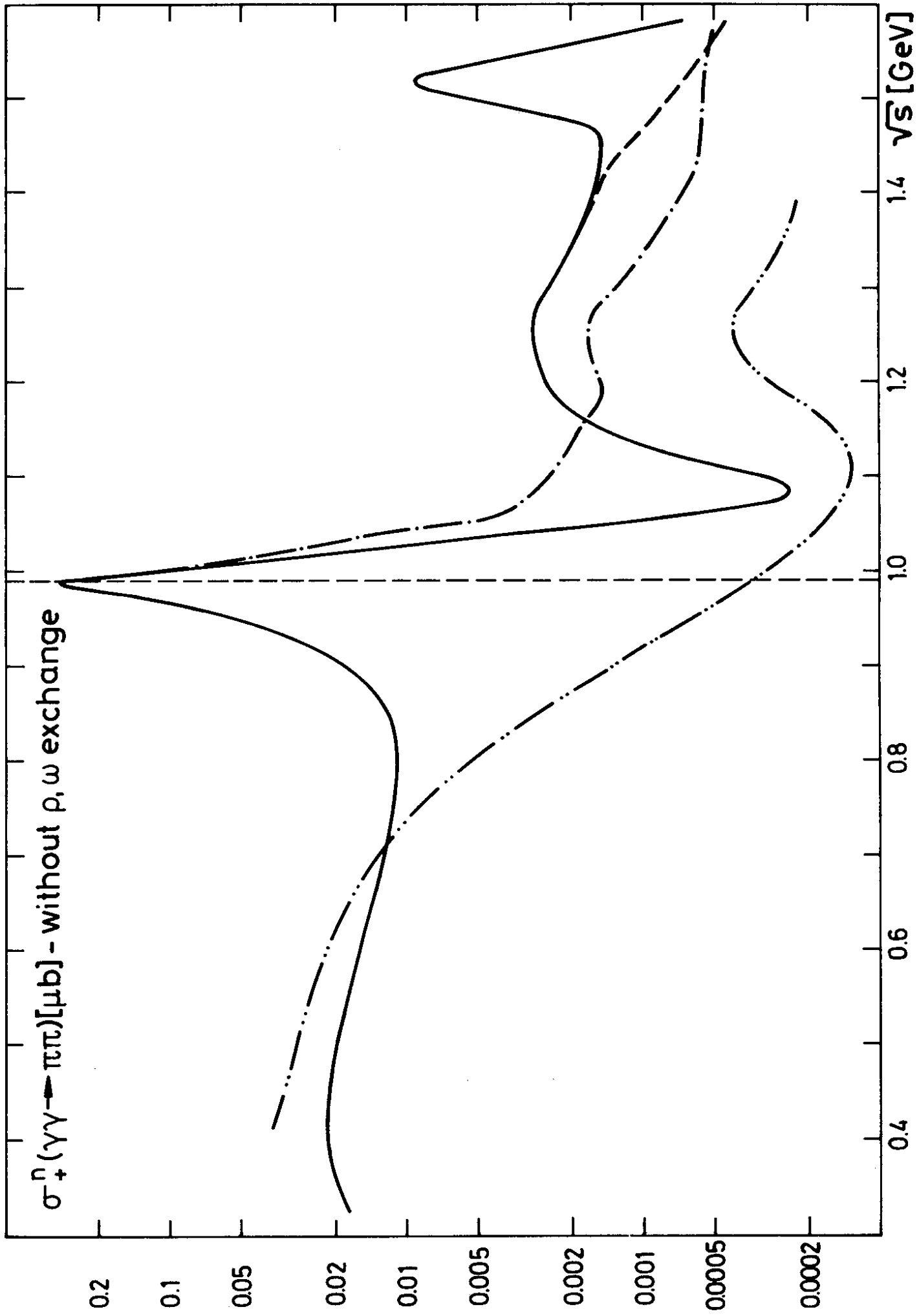


Fig. 8

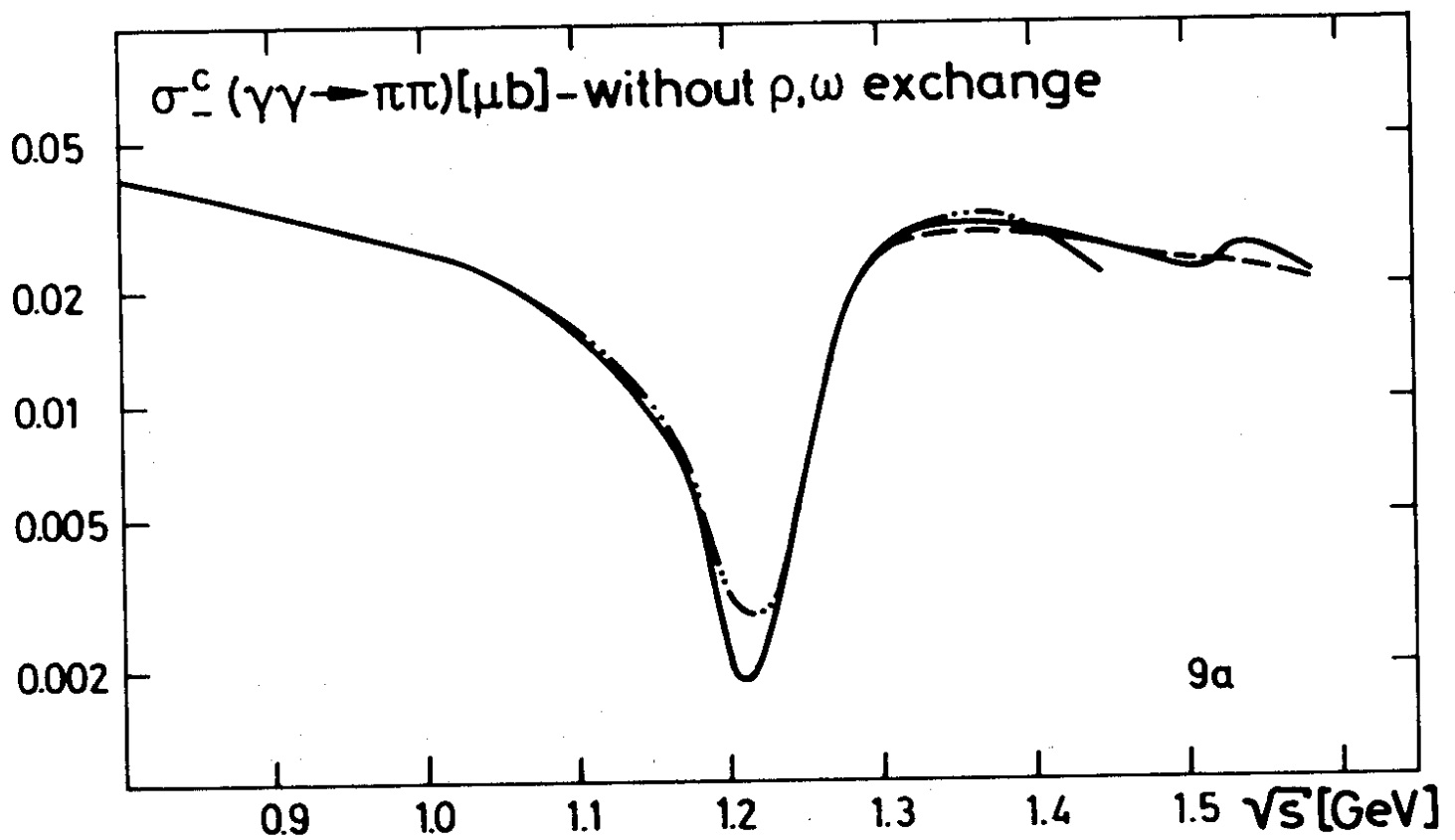
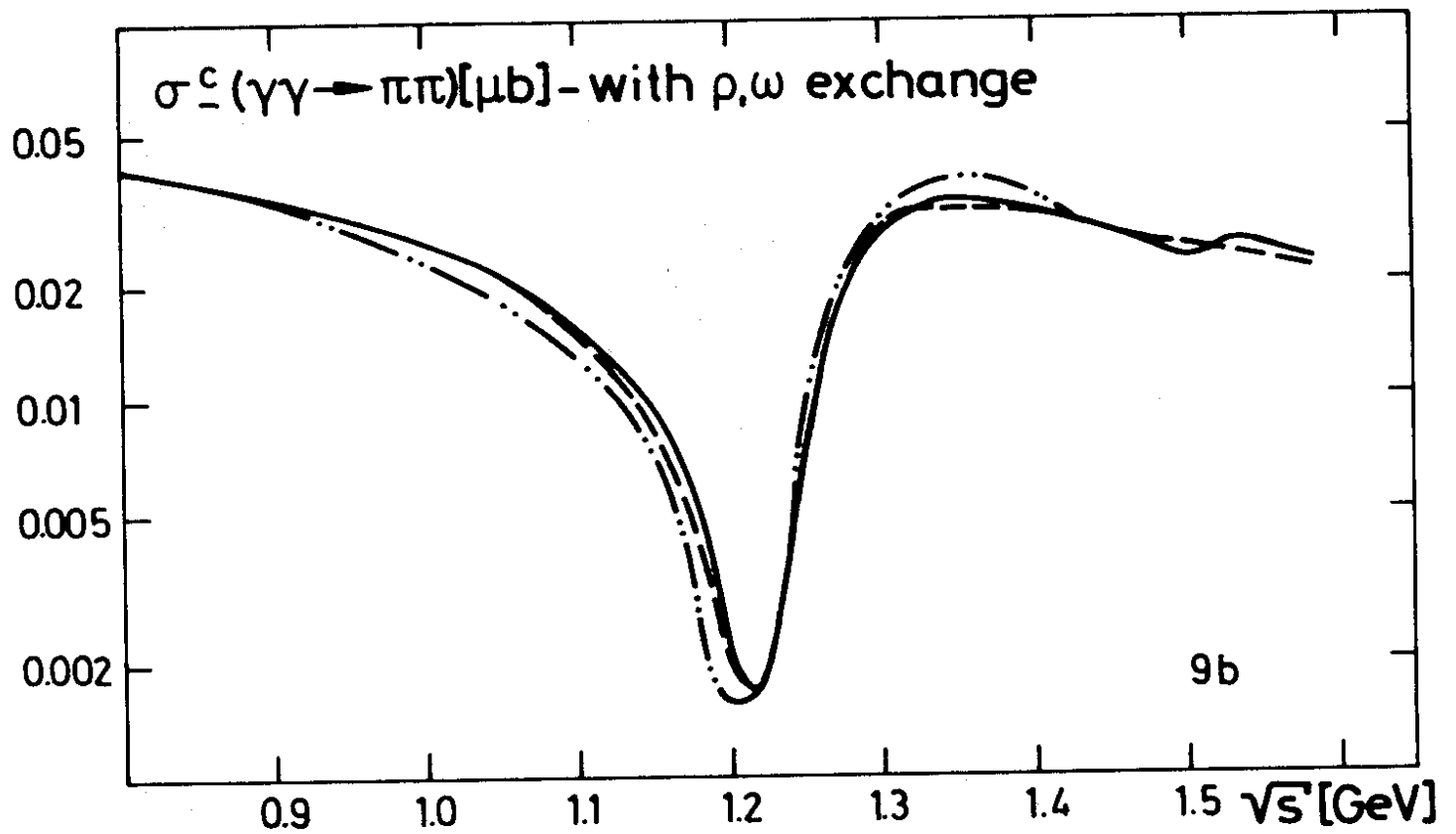


Fig. 9

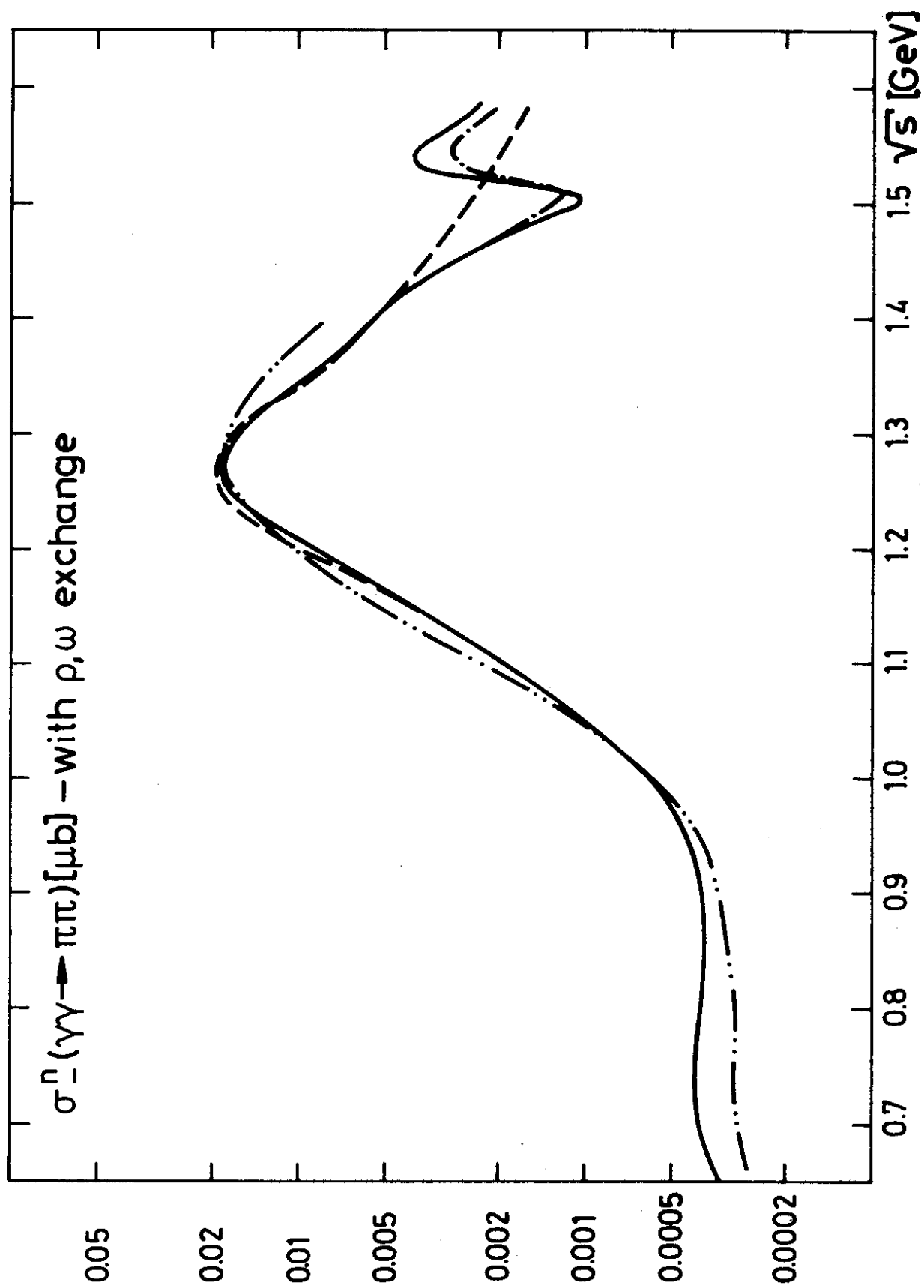


Fig.10

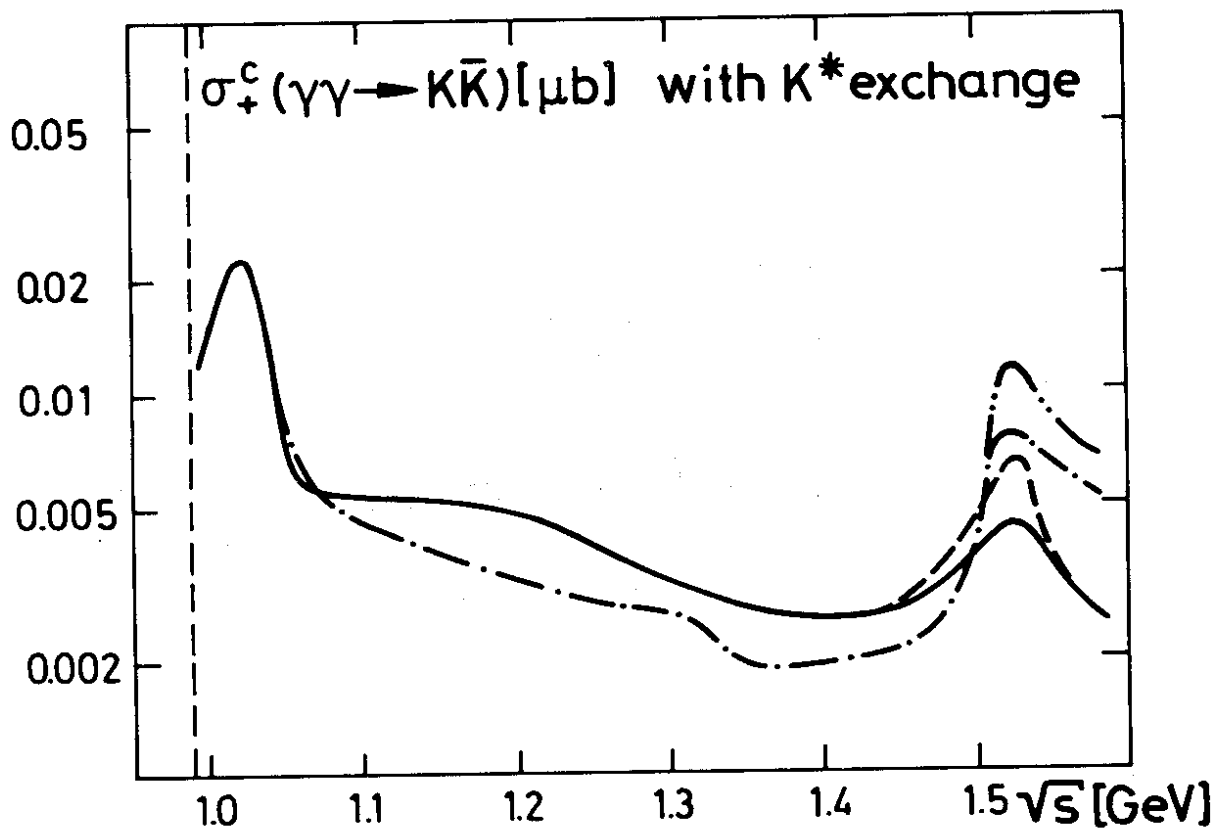


Fig. 11a

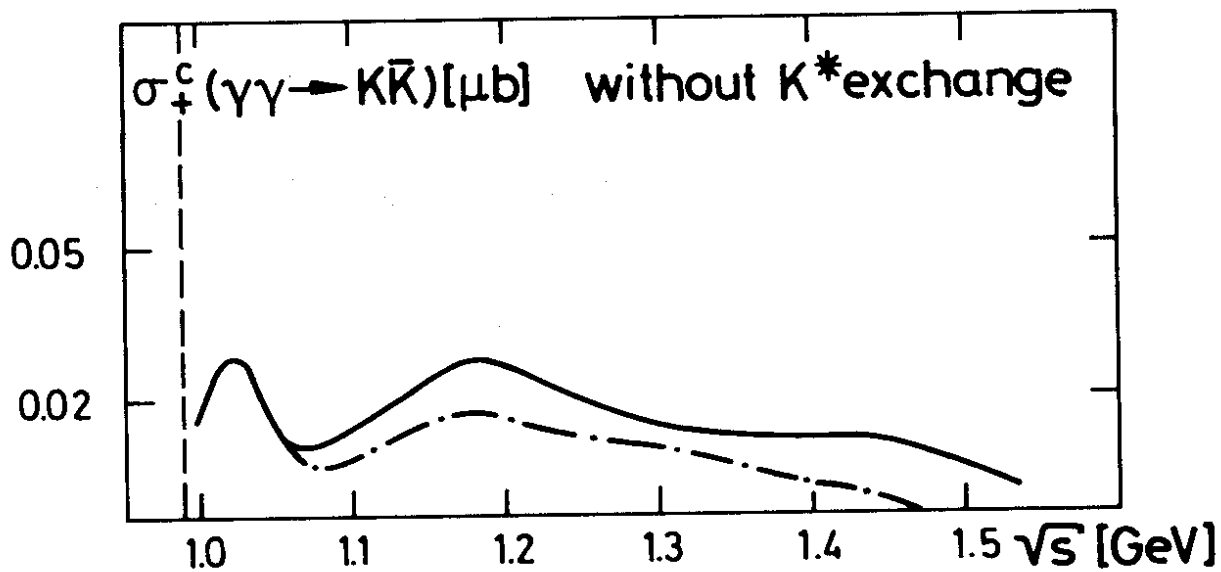


Fig. 11b

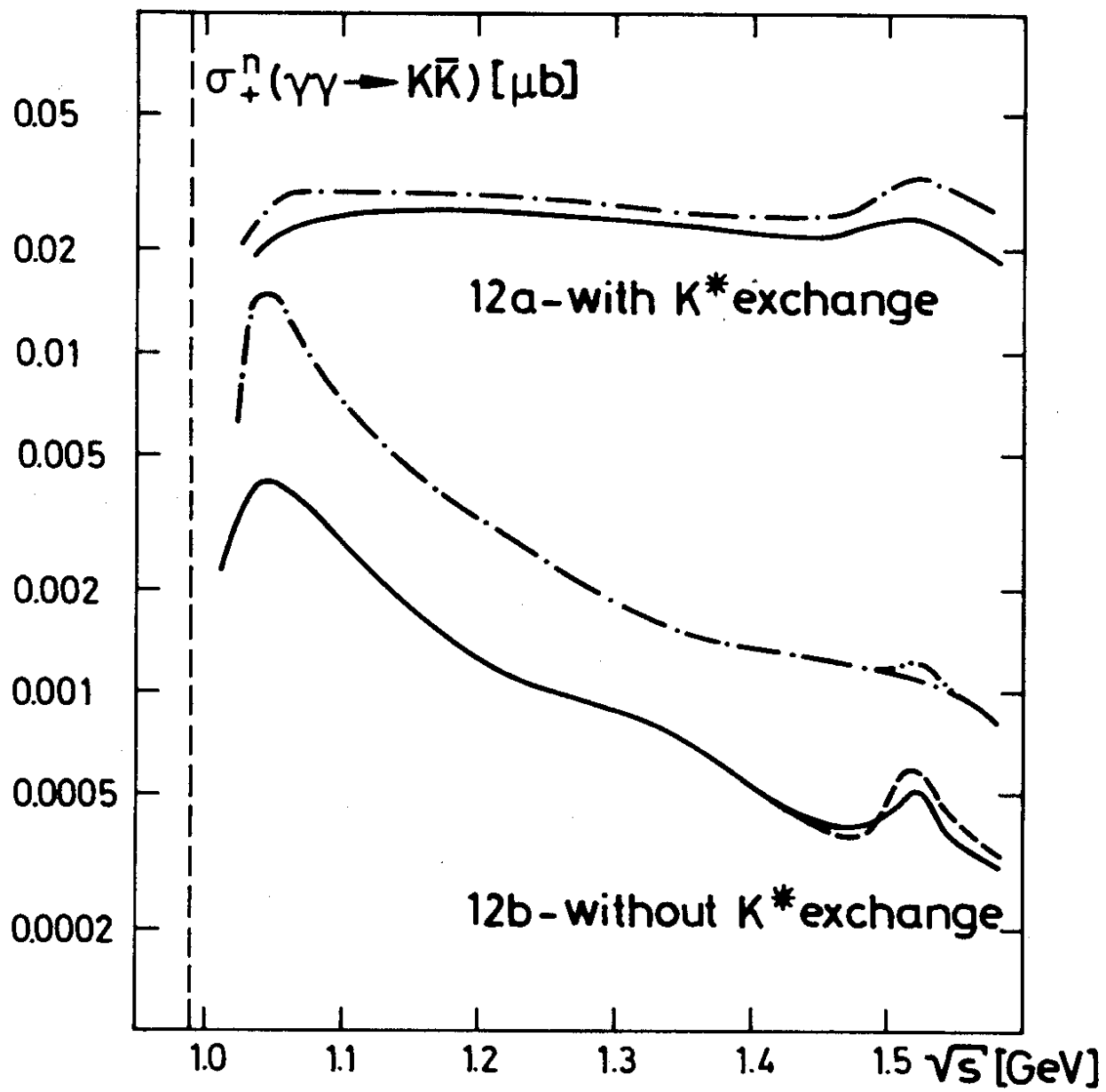


Fig. 12

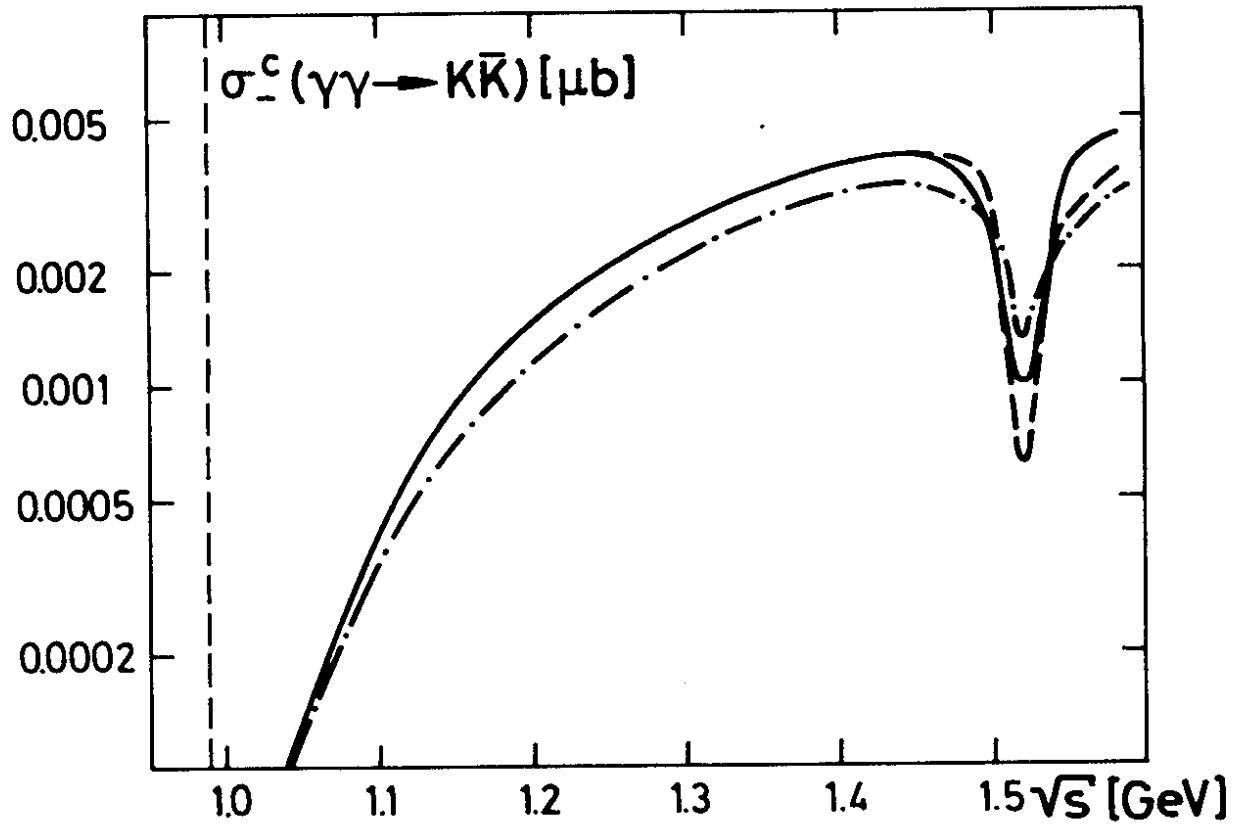


Fig. 13

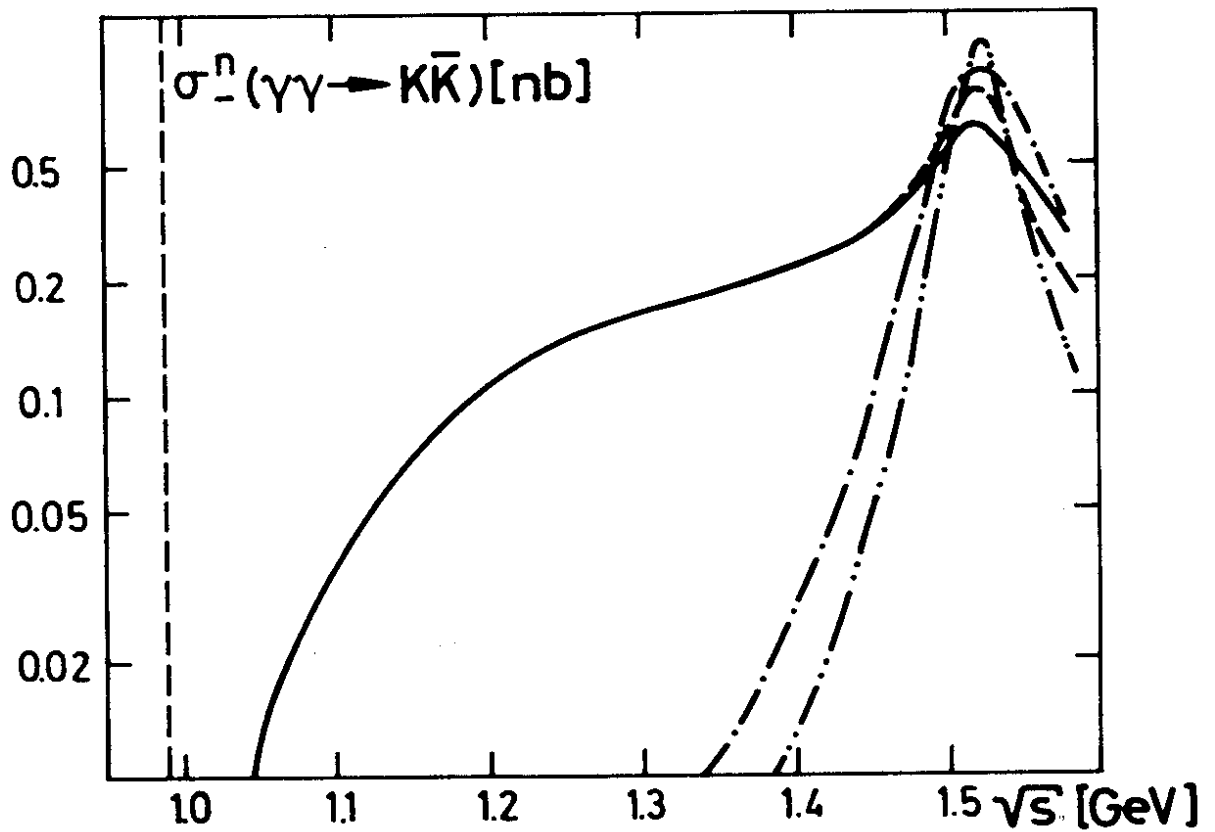


Fig. 14